Pertanika J. Trop. Agric. Sci. 49 (5): 2275 - 2302 (2026)

PERTANIKA JOURNALS

TROPICAL AGRICULTURAL SCIENCE

Journal homepage: http://www.pertanika.upm.edu.my/

Visible-Near Infrared Spectroscopy for Predicting Carotenoid and Antioxidant Composition in Healthy and Bronzed Jackfruit (*Artocarpus heterophyllus* Lam. cv. Tekam Yellow) at Different Maturity Stages

Kok Jeng Lim[1]*, Phebe Ding[1], Nazmi Mat Nawi[2,3], and Mashitah Jusoh[1]

[1]*Department of Crop Science, Faculty of Agriculture, Universiti Putra Malaysia, 43400 UPM Serdang, Selangor Malaysia*

[2]*Department of Biological and Agricultural Engineering, Faculty of Engineering, Universiti Putra Malaysia, 43400 UPM Serdang, Selangor, Malaysia*

[3]*Institute of Plantation Studies, Universiti Putra Malaysia, 43400 UPM Serdang, Selangor, Malaysia*

ABSTRACT

Jackfruit bronzing disease (JBD), associated with *Pantoea stewartii* subsp. *stewartii*, is a quality disorder in Malaysian jackfruit that causes internal discoloration without obvious changes to the rind. This study evaluated visible-near infrared spectroscopy (Vis-NIRS) for predicting selected carotenoid and antioxidant-related attributes in intact jackfruit cv. Tekam Yellow at 10, 12, and 14 weeks after anthesis (WAA). Reflectance spectra were collected at 30 rind locations per fruit within the 500–950 nm range. Partial least squares regression (PLSR) models were developed using alternative spectral preprocessing methods. Flesh β-carotene, lycopene, total flavonoid content (TFC), and total phenolic content (TPC) served as reference variables. Prediction performance varied according to maturity stage, fruit condition, target attribute, and spectral preprocessing. Among healthy fruit, the β-carotene model at 12 WAA achieved an Rp^2 of 0.88 and a residual predictive deviation (RPD) of 4.12, while the TFC model at 10 WAA yielded an Rp^2 of 0.98 and an RPD of 43.17. For bronzing-affected fruit at 14 WAA, the lycopene model achieved an Rp^2 of 0.94 and an RPD of 12.36, although this high RPD should be interpreted alongside prediction error and validation-data distribution. At 12 WAA, TPC models achieved Rp^2 values of 0.87 and 0.92 for healthy and bronzing-affected fruit, respectively, with corresponding RPD values of 3.57 and 2.54. Spectral regions near 760 and 945 nm contributed to several models. Overall, rind-based Vis-NIRS demonstrated potential

ARTICLE INFO

Article history:
Received: 26 June 2026
Accepted: 17 September 2026
Published: 30 October 2026

DOI: https://doi.org/10.47836/pjtas.49.5.09

E-mail addresses:
limkokjeng@gmail.com (Kok Jeng Lim)
phebe@upm.edu.my (Phebe Ding)
nazmimat@upm.edu.my (Nazmi Mat Nawi)
mashitahj@upm.edu.my (Mashitah Jusoh)
* Corresponding author

© Universiti Putra Malaysia Press

for predicting selected internal biochemical attributes under specific maturity and fruit-condition combinations, although performance varied among models.

Keywords: Carotenoids, flavonoid, jackfruit bronzing disease, partial least squares regression, phenolics, visible-near infrared spectroscopy

INTRODUCTION

Jackfruit (*Artocarpus heterophyllus* Lam.) is an important tropical fruit crop widely grown in South and Southeast Asia and a key source of income for smallholder growers. In Malaysia, cv. Tekam Yellow is commercially valued for its yellow flesh colour, characteristic aroma, relatively high soluble solids content, and firm aril texture, which make the fruit suitable for both fresh consumption and processing (Mijin & Ding, 2020). Production of this cultivar has increased with market demand, further highlighting its importance to the local jackfruit industry (Mijin et al., 2021; Lim et al., 2026a). Despite this, obtaining fruit with consistent maturity and internal quality remains difficult because the fruit's internal condition cannot always be accurately judged from its external appearance.

Jackfruit maturity is generally assessed using visible or sensory characteristics, including spine development and flattening, rind colour, leaf condition, and aroma. These characteristics are useful in practice, but their appearance can vary with orchard and environmental conditions, which may lead to differences in harvest maturity and eating quality (Jarman et al., 2023; Lim et al., 2026a). As the fruit develops, its chemical composition also changes. Pigments such as β-carotene and lycopene contribute to the characteristic colour of the edible tissues, while flavonoids and phenolic compounds form part of the antioxidant profile of the fruit. Changes in these compounds therefore provide useful information about the biochemical condition of the fruit during development.

Jackfruit bronzing disease (JBD) presents an additional quality problem in Malaysian production. The disease has been associated with *Pantoea stewartii* subsp. *stewartii* (Zulperi et al., 2017; Abidin et al., 2020) and is characterised by brownish to reddish discoloration within the edible tissues. In some affected fruits, the external rind shows little or no obvious indication of the internal disorder. This makes visual inspection alone unreliable for determining whether an apparently normal fruit is affected internally. Bronzing disease has also been reported in other jackfruit-producing regions, including China (Zhao et al., 2023; Abidin et al., 2021). A method that can provide information about internal fruit quality without cutting the fruit would therefore be useful for jackfruit quality assessment.

Visible-near infrared spectroscopy (Vis-NIRS) has been used to obtain information about fruit quality from spectral measurements taken without destructive sampling. The technique has been applied to intact and structurally complex fruits for estimating physicochemical properties and for studying physiological changes. For jackfruit, previous

work has shown that spectral information obtained from the fruit surface can be used to estimate attributes such as moisture and soluble solids content (Abdullah, 2019; Abdullah et al., 2018, 2021). Studies on other tropical and structurally complex fruits, including durian, kiwifruit, and mango, have also reported relationships between surface spectra and internal quality attributes (Clark et al., 2004, 2022; Li et al., 2023; Saechua et al., 2021).

However, using spectra collected from the rind to estimate biochemical properties measured inside a thick-skinned fruit such as jackfruit is not straightforward. The spectrum obtained from the rind should not be regarded as a direct measurement of the compounds present in the internal flesh. Instead, the relationship may arise from changes that occur together during fruit development or disease progression, including differences in tissue composition, water status, structural characteristics, and other physiological processes. Therefore, in this study, rind-based Vis-NIRS is treated as an indirect prediction method, where spectral information collected externally is related statistically to reference measurements of internal biochemical attributes.

Another consideration is the variation in rind structure across the surface of an intact jackfruit. A single scanning point may not adequately represent the spectral variability of the whole fruit. Collecting spectra from several locations can provide a broader representation of this surface variability and has been applied in studies involving heterogeneous fruit matrices (Li et al., 2023). Nevertheless, the use of multiple rind positions to relate surface spectral variation to internal biochemical attributes in healthy and bronzing-affected jackfruit has received limited attention.

The present study was designed to address this gap by examining both the biochemical variation associated with maturity and fruit condition and the usefulness of multi-position rind-based Vis-NIRS for prediction. β-Carotene, lycopene, total flavonoid content (TFC), and total phenolic content (TPC) were measured in healthy and bronzing-affected cv. Tekam Yellow fruit harvested at 10, 12, and 14 weeks after anthesis (WAA). Vis-NIR spectra collected from the rind were then used to develop partial least squares regression (PLSR) models. The effects of spectral preprocessing, maturity stage, and fruit condition on model performance were also examined.

The study was based on the expectation that biochemical changes occurring during fruit maturation and bronzing development may be accompanied by measurable changes in the rind spectral response. The specific objectives were to: (i) characterise maturity- and bronzing-associated changes in selected carotenoid and antioxidant-related attributes of Tekam Yellow jackfruit; (ii) evaluate multi-position rind-based Vis-NIRS for predicting these internal attributes using PLSR; and (iii) determine the spectral preprocessing and modelling conditions that provided useful prediction performance for healthy and bronzing-affected fruit. The results are intended to provide a basis for further work on non-destructive assessment of maturity- and bronzing-associated quality variation in jackfruit.

MATERIALS AND METHODS

Plant Material and Harvesting Stages

Jackfruit (*Artocarpus heterophyllus* Lam.) cv. Tekam Yellow was obtained from a commercial plantation operated by Agro BS Sdn. Bhd. in Jasin, Melaka, Malaysia (2°23′31.50″ N, 102°25′7.48″ E). Fruit sampling was carried out over three harvesting seasons, which were treated as three independent batches. A total of 54 syncarps were collected. Both healthy and bronzing-affected fruits were sampled at 10, 12, and 14 weeks after anthesis (WAA), with six fruits collected at each maturity stage in each batch.

The three harvesting stages were selected to represent different points of fruit development and to capture changes in biochemical composition associated with maturity and bronzing. The WAA of each fruit was determined from the anthesis records maintained at the plantation. After harvesting, the fruits were placed in plastic sacks and handled carefully to avoid unnecessary mechanical damage. The fruits were transported to the laboratory at Universiti Putra Malaysia within 2 hours of harvest for spectral measurements and subsequent chemical analysis.

Spectral Data Collection

Visible-near infrared (Vis-NIR) spectra were collected using an Ocean Optics HR4000 spectrometer (Ocean Optics Inc., Winter Park, FL, USA), which covers the 200-1100 nm wavelength range. For the multivariate analysis, the spectral region from 500 to 950 nm was used. Measurements were made in reflectance mode with a 1.5-cm scanning aperture.

Each intact fruit was measured at 30 locations on the rind. The measurement locations were distributed among five latitudinal zones: top (A), middle-top (B), middle (C), middle-bottom (D), and bottom (E). Six positions were measured within each zone (A1-A6, B1-B6, C1-C6, D1-D6, and E1-E6), giving 30 scanning positions per fruit. This arrangement was used to capture variation across the rind surface rather than relying on a single measurement location.

The HL-2000 halogen light source (Ocean Optics Inc., USA) was allowed to warm up for at least 30 min before measurements were started. A white reference standard, corresponding to approximately 100% reflectance, was recorded before each measurement session. Three spectra were collected at each position and averaged to obtain one representative spectrum for that location. Measurements were made inside a black chamber using a fibre-optic probe connected to the spectrometer and light source. The probe was placed directly against the rind surface during scanning. The measurements were carried out in a darkened room to minimise the effect of ambient light.

The decision to collect spectra from the rind was based partly on previous jackfruit studies showing that surface measurements can provide information related to physicochemical properties. Abdullah (2019) examined shortwave near-infrared

spectroscopy for jackfruit physicochemical properties, while Abdullah *et al*. (2018, 2021) reported the prediction of moisture content and soluble solids content using spectra collected from the peel surface. In the present study, spectra collected from the rind were paired with destructive measurements from the corresponding fruit tissues so that their statistical relationship with internal biochemical attributes could be examined.

Reference Methods

Determination of Flesh Carotenoids

Carotenoids were extracted following the procedure of Nagata and Yamashita (1992), with minor modifications. Approximately 5 g of fresh jackfruit flesh was homogenised with 50 mL of chilled acetone using a high-speed blender (Model MX V2N, National, Malaysia) for 1 min. The homogenate was then filtered through Whatman No. 1 filter paper. A 20-mL portion of the filtrate was transferred to a separate container and mixed with 20 mL of petroleum ether. Distilled water (5 mL) was then added to facilitate phase separation. The upper petroleum ether layer was collected, and its absorbance was measured at 663, 645, 505, and 453 nm using a UV-Visible spectrophotometer.

The concentrations of β-carotene and lycopene were calculated using the following Equations 1 and 2:

$$\textbf{β-carotene (mg/100 mL of extract)} = 0.216 \times A663 - 1.22 \times A645 - 0.304 \times A505 + 0.452 \times A453 \quad [1]$$

$$\textbf{Lycopene (mg/100 mL of extract)} = -0.0458 \times A663 + 0.204 \times A645 + 0.372 \times A505 - 0.0806 \times A453 \quad [2]$$

The carotenoid concentrations were expressed as milligrams per kilogram of fresh weight (mg/kg FW).

Assessment of Flesh Antioxidant Contents

Fresh jackfruit flesh was cut into approximately 1-cm³ pieces and homogenised using a food blender (Model MX V2N, National, Malaysia). A 1-g portion of the homogenised sample was extracted with 10 mL of 50% (v/v) methanol. The mixture was centrifuged at 4750 rpm for 10 min using a tabletop centrifuge (Model 1370R, Scanspeed, Denmark). The resulting supernatant was collected and used for the determination of total flavonoid content (TFC) and total phenolic content (TPC). The remaining extract was stored at -20°C until analysis.

Total Flavonoid Content. Total flavonoid content was measured using the colorimetric procedure adapted from Abu Bakar et al. (2009). An aliquot of 0.5 mL of extract was mixed with 2.25 mL of distilled water and 0.15 mL of 5% (w/v) sodium nitrite ($NaNO_3$). After 6 min, 0.3 mL of 10% (w/v) aluminium chloride ($AlCl_3$) was added and allowed to react for another 5 min. Then, 1.0 mL of 1 M sodium hydroxide (NaOH) was added. Absorbance was measured at 510 nm using a UV-Visible spectrophotometer (Multiskan Go, Thermo Fisher Scientific, UK). Quercetin was used as the calibration standard, and the results were expressed as milligrams of quercetin equivalents per gram of fresh weight (mg QE/g FW), as shown in Equation 3.

$$= \frac{\text{QE equivalent} \times \text{volume of fresh jackfruit extract} \times \text{dilution jackfruit extract}}{\text{weight of jackfruit flesh used}} \quad [3]$$

Total Phenolic Content. Total phenolic content was determined using the Folin-Ciocalteu procedure described by Musa et al. (2011), with slight modifications. A 0.5-mL aliquot of extract was mixed with 0.4 mL of distilled water and 0.1 mL of diluted Folin-Ciocalteu reagent. After 5 min, 1.0 mL of 7.5% (w/v) sodium carbonate (Na_2CO_3) was added. The mixture was kept at room temperature in the dark for 2 h. Absorbance was then measured at 765 nm using a UV-Visible spectrophotometer. Gallic acid was used as the calibration standard, and the results were expressed as milligrams of gallic acid equivalents per gram of fresh weight (mg GAE/g FW) in Equation 4.

$$= \frac{\text{GAE equivalent} \times \text{volume of fresh jackfruit extract} \times \text{dilution jackfruit extract}}{\text{weight of jackfruit flesh used}} \quad [4]$$

Multivariate and Statistical Analyses

Spectral data were analysed using Unscrambler X version 10.3 (CAMO AS, Oslo, Norway). The dataset was separated into calibration and external validation subsets using a 75:25 independent sample-level split. The calibration subset was used to build the models, while the validation subset was kept separate for evaluating external prediction performance. Leave-one-out cross-validation was carried out within the calibration subset to examine model stability (Ali et al., 2021; Sirisomboon & Nawayon, 2017).

Before the data were divided, the samples were arranged in ascending order according to their reference chemical values. The software was then used to make the random selection of calibration and validation samples. Importantly, the separation was made at the fruit level.

Thus, spectra obtained from the same fruit were not placed in both the calibration and external validation subsets, reducing the possibility of information leakage between the two datasets.

Several spectral preprocessing procedures were examined to reduce variation associated with the heterogeneous rind surface, including the effects of rind roughness and spine density. The evaluated procedures included Savitzky-Golay smoothing, baseline correction, median filtering, Gaussian filtering, standard normal variate (SNV), and multiplicative scatter correction (MSC), together with the combinations used in the analysis. Similar preprocessing approaches have been applied in Vis-NIR studies of intact fruit quality (Abdullah et al., 2021; Lim et al., 2026b, 2026d).

Partial least squares regression (PLSR) was used to relate the rind spectral data to the reference measurements obtained from the flesh. The models were developed using the 500-950 nm spectral interval. Approximately 5% of extreme spectral outliers were removed before modelling to minimise the influence of noise and anomalous measurements (Abdullah, 2019). After this screening step, 1,620 valid spectra remained, representing 30 scanning positions from each of the 54 fruits.

Model performance was examined using the coefficient of determination for calibration (R^2c), cross-validation (R^2cv), and external validation (Rp^2). The corresponding root means square errors for calibration (RMSEc), cross-validation (RMSEcv), and prediction (RMSEp), together with bias and residual predictive deviation (RPD), were also considered. These measures were evaluated together to describe the agreement between predicted and reference values and the stability of the models (Sirisomboon & Nawayon, 2017).

The performance indices were calculated using the following Equations 5 to 9:

$$R^2 = \frac{\sum_{i=1}^{n}(\hat{y}\mathrm{i} - \mathrm{yi})^2}{\sum_{i=1}^{n}(\hat{y}\mathrm{i} - \mathrm{ym})^2} \quad [5]$$

$$RMSEV = \sqrt{\frac{1}{\mathrm{nv} - 1}\sum_{i=1}^{nv}(\hat{y}\mathrm{i} - \mathrm{yi} - \mathrm{bias})^2} \quad [6]$$

$$RMSEC = \sqrt{\frac{1}{\mathrm{nc} - 1}\sum_{i=1}^{nc}(\hat{y}\mathrm{i} - \mathrm{yi})^2} \quad [7]$$

$$Bias = \frac{1}{\mathrm{nv}}\sum_{i=1}^{nv}(\hat{y}\mathrm{i} - \mathrm{yi}) \quad [8]$$

$$RPD = \frac{\text{SD}}{\text{RMSEP}} \quad [9]$$

Where n is the number of data samples, n_c is the number of data samples for calibration, n_v is the number of data samples for validation, $\hat{y}_i$ is the prediction value, y_i is the measured value and y_m is the mean value.

PLSR models were developed for β-carotene, lycopene, TFC, and TPC using the evaluated spectral preprocessing procedures. The number of latent variables (LVs) was tested sequentially from 1 to 7. This range was used to obtain suitable model complexity while limiting the possibility of overfitting, following Peirs et al. (2003) and Saechua et al. (2021).

The experiment followed a completely randomised design with three replications. Analysis of variance (ANOVA) was used to examine treatment effects, and mean comparisons were performed using Fisher's protected least significant difference (LSD) test at $p \leq 0.05$. Statistical analyses were conducted using R version 4.0.4.

RESULT

Distribution of Calibration and Prediction Reference Data

Carotenoid Dynamics Across Fruit Conditions and Maturity Stages

ß-Carotene. The β-carotene content of jackfruit flesh was significantly affected by the interaction between weeks after anthesis (WAA) and fruit condition (Table 1). The concentration changed across the three maturity stages and showed an overall decrease at

Table 1
Main and interaction effects of week after anthesis and fruit condition on the flesh ß-carotene and lycopene of jackfruit cv. Tekam Yellow.

Factor	ß-carotene (mg/kg FW)	Lycopene (mg/kg FW)
Harvest ae (WAA)		
W10	4.51b[x]	3.02b
W12	5.52a	3.79a
W14	3.91b	2.54b
Quality Condition (H)		
Asymptomatic (N)	5.36a	3.51a
Symptomatic (B)	4.02b	2.77b
Interaction		
WAA × H	**	-

Note. [x] For each factor, mean comparisons within the factors followed by different letters are significantly different by LSD at p≤0.05. NS, **, non-significant at p>0.05 or highly significant at p≤0.01, respectively

the later stage of fruit development (Figure 1). At 12 and 14 WAA, normal fruits contained significantly higher β-carotene concentrations than bronzing-affected fruits. The difference between the two fruit conditions became more apparent at the later maturity stages, indicating that the effect of fruit condition was dependent on the stage of fruit development.

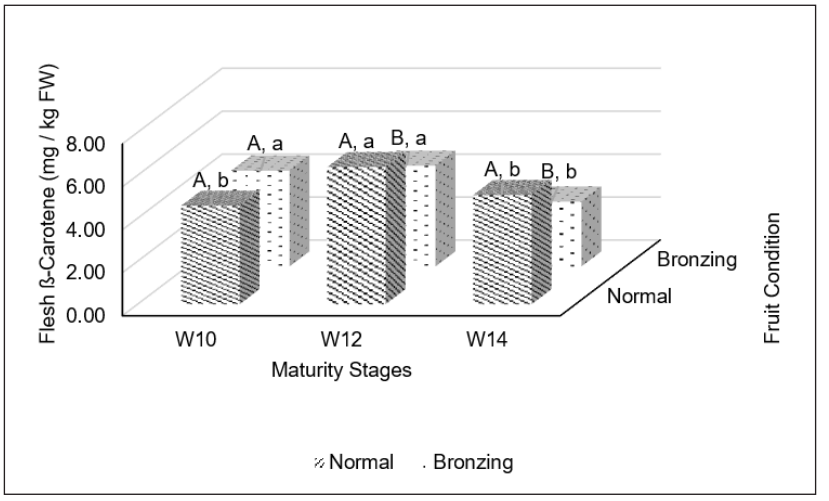

Figure 1. Effects of fruit condition and maturity stages (weeks after anthesis) on flesh ß-carotene of jackfruit cv. Tekam Yellow. Means separated by different capital and small letters are significantly different ($p \leq 0.05$) using LSD between fruit condition and maturity stages, respectively

Lycopene. The interaction between WAA and fruit condition did not significantly affect lycopene concentration (Table 1). Maturity stage, however, had a significant effect, with lycopene concentration decreasing at the later stages of development. Although the interaction was not significant, bronzing-affected fruits showed lower mean lycopene concentrations than normal fruits across the maturity stages. Thus, the difference between fruit conditions was observed in the measured means, but the magnitude of this difference did not change sufficiently across maturity stages to result in a significant interaction.

Antioxidant Contents across Fruit Conditions and Maturity Stages

Total Flavonoid Content. A significant interaction between WAA and fruit condition was found for total flavonoid content (TFC) (Table 2). The pattern changed with maturity. At 10 WAA, normal fruits had higher TFC than bronzing-affected fruits. At 12 and 14 WAA, this pattern was reversed, with bronzing-affected fruits showing higher mean TFC values (Figure 2). These results indicate that the relationship between fruit condition and TFC changed during fruit development.

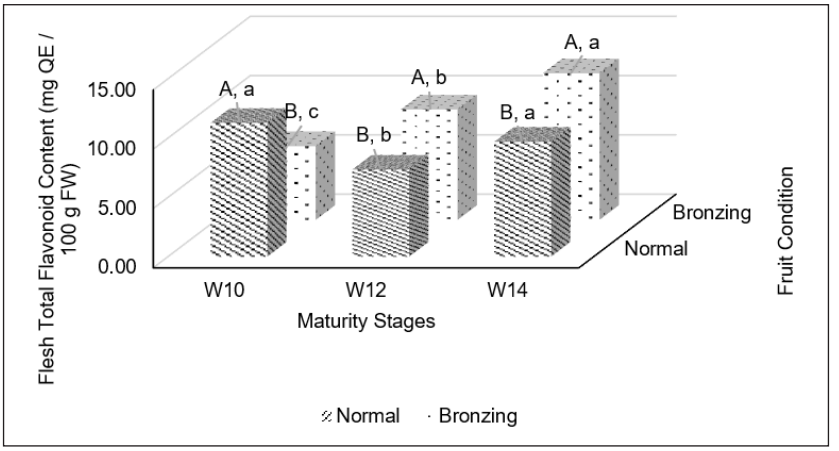

Figure 2. Effects of fruit condition and maturity stages (weeks after anthesis) on flesh total flavonoid content of jackfruit cv. Tekam Yellow. Means separated by different capital and small letters are significantly different ($p \leq 0.05$) using LSD between fruit condition and maturity stages, respectively

Table 2
Main and interaction effects of week after anthesis and fruit condition on the flesh total flavonoid content and total phenolic content of jackfruit cv. Tekam Yellow

Factor	Total Flavonoid Content (mg QE / 100 g FW)	Total Phenolic Content (mg GAE / 100 g FW)
Weeks after anthesis (WAA)		
10	8.39b[x]	3.52c
12	8.30b	6.14a
14	11.14a	4.51b
Fruit Condition (H)		
Normal (N)	9.37a	5.26a
Bronzing (B)	9.21a	4.19b
Interaction		
WAA × H	***	***

Note. [x] For each factor, mean comparisons within the factors followed by different letters are significantly different by LSD at $p \leq 0.05$. ***, highest significant at $p \leq 0.001$, respectively

Total Phenolic Content. Total phenolic content (TPC) was also significantly affected by the interaction between WAA and fruit condition (Table 2). In normal fruits, TPC decreased from 10 to 14 WAA, whereas the values for bronzing-affected fruits were comparatively less variable across the maturity stages. Normal fruits had lower TPC than bronzing-affected fruits at 10 WAA but higher values at 12 WAA (Figure 3). The results therefore show that the difference in TPC between the two fruit conditions was not consistent throughout fruit development.

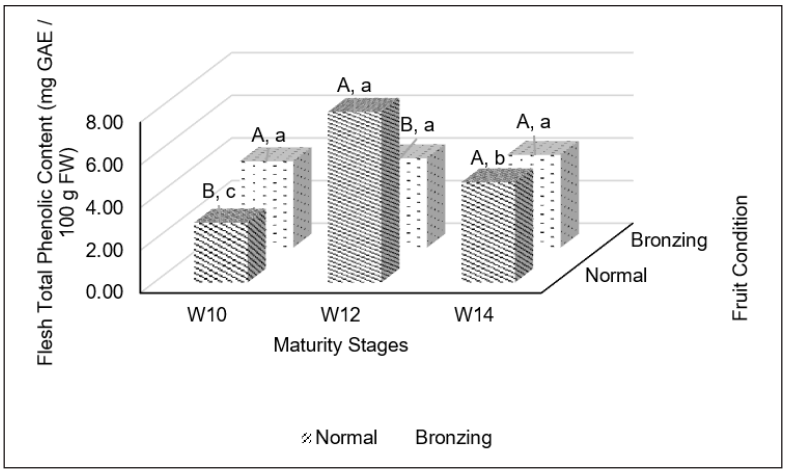

Figure 3. Effects of fruit condition and maturity stages (weeks after anthesis) on flesh total phenolic content of jackfruit cv. Tekam Yellow. Means separated by different capital and small letters are significantly different ($p \leq 0.05$) using LSD between fruit condition and maturity stages, respectively

Spectral Characteristics of Jackfruit Peel

Figures 4 and 5 present the raw Vis-NIR reflectance spectra of normal and bronzing-affected jackfruit rinds at 14 WAA, while Figures 6 and 7 show the corresponding preprocessed spectra. The spectra were obtained from 1,620 valid spectral observations. Broad and overlapping features were observed throughout the measured spectral range, which is expected for fruit tissues because the recorded response can contain contributions from several molecular vibration bands (Nicolaï et al., 2007).

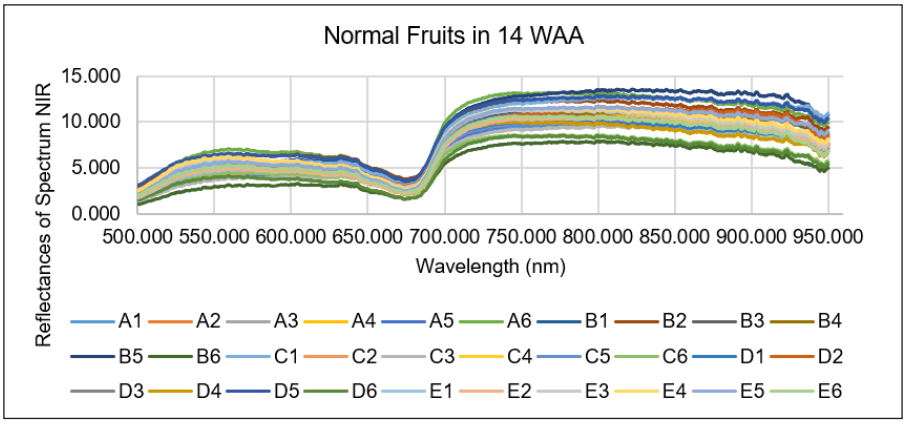

Figure 4. Mean spectral reflectance of raw material for healthy fruit of 30 portions at 14 WAA

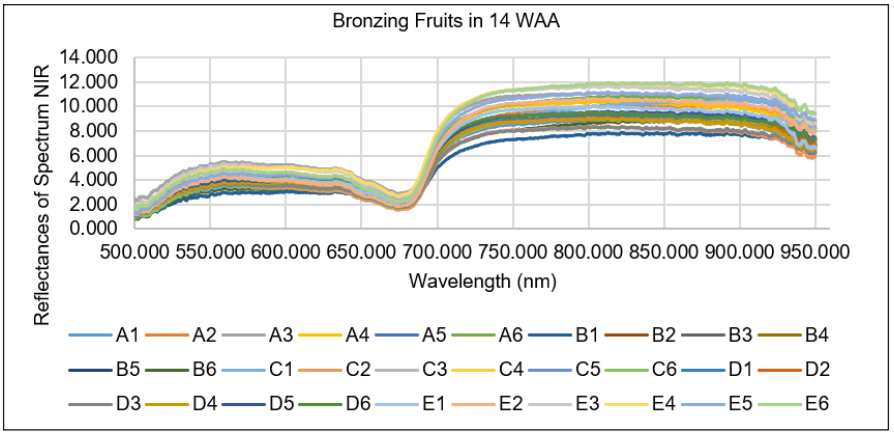

Figure 5. Mean spectral reflectance of raw material for bronzing-affected fruit of 30 portions at 14 WAA

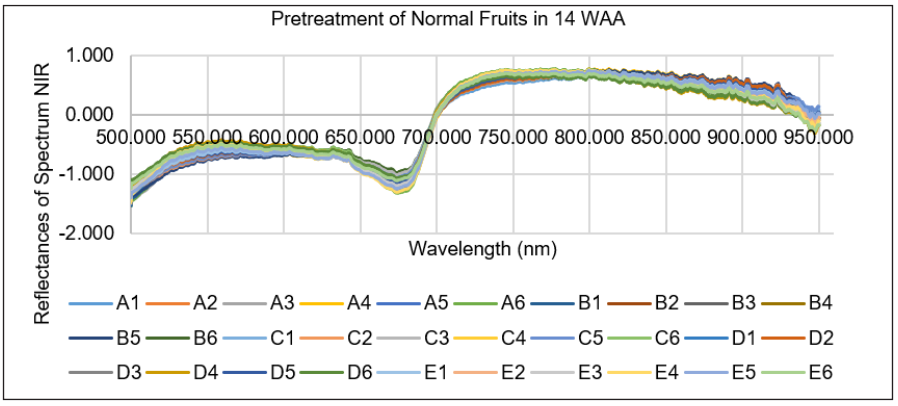

Figure 6. Preprocessed mean Vis-NIR reflectance spectra of healthy jackfruit rind at 14 WAA (30 portions) after Savitzky-Golay smoothing and SNV correction

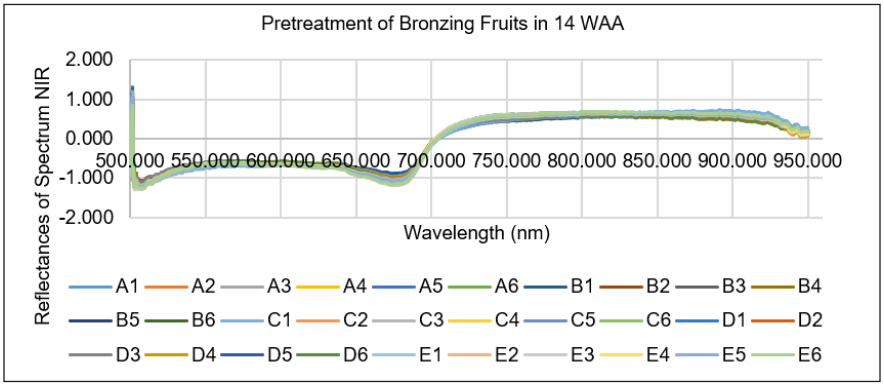

Figure 7. Preprocessed mean Vis-NIR reflectance spectra of bronzing-affected jackfruit rind at 14 WAA (30 portions) after Savitzky-Golay smoothing and SNV correction

The mean spectra obtained from the 30 scanning positions per fruit also showed variation among rind regions. The measurement positions covered five zones: top (A1-A6), middle-top (B1-B6), middle (C1-C6), middle-bottom (D1-D6), and bottom (E1-E6). Using all five zones allowed the spectral dataset to include variation across the heterogeneous rind surface.

Both normal and bronzing-affected rinds showed features around 675 and 945 nm, together with a broader response near 970 nm. The feature around 970 nm is associated mainly with O-H-related absorption and has been reported in fruit tissues (Nagy et al., 2016). The 940-970 nm region may also contain contributions from soluble constituents in fruit materials (Babu et al., 2020; Maniwara et al., 2014). Because the final modelling range was limited to 500-950 nm, the region around 970 nm was not included in the PLSR models.

Within the selected 500-950 nm range, responses around approximately 760 and 945 nm were visible. The raw spectra also showed baseline shifts and scattering effects. These features became less pronounced after spectral preprocessing, particularly after smoothing and SNV correction, resulting in more stable baseline profiles.

Regression coefficient plots for the selected models (Figures 8-15) showed influential regions around 754-760 nm and toward 945 nm. These wavelength regions should not be treated as specific spectral fingerprints of β-carotene, lycopene, TFC, TPC, or bronzing. Instead, they represent parts of the spectrum that contributed to the statistical relationships between the rind spectra and the biochemical measurements obtained from the flesh.

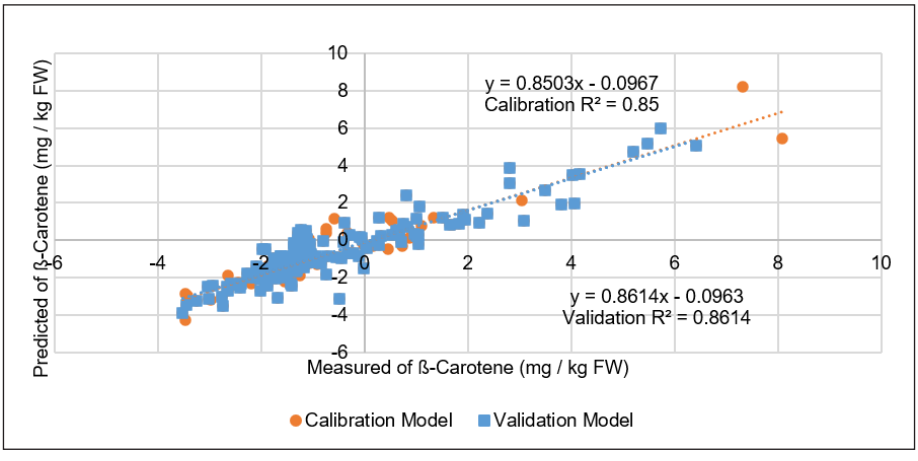

Figure 8. Scatter plots of measured versus predicted β-carotene concentrations in normal jackfruit flesh at 12 weeks after anthesis using Vis-NIR reflectance spectra

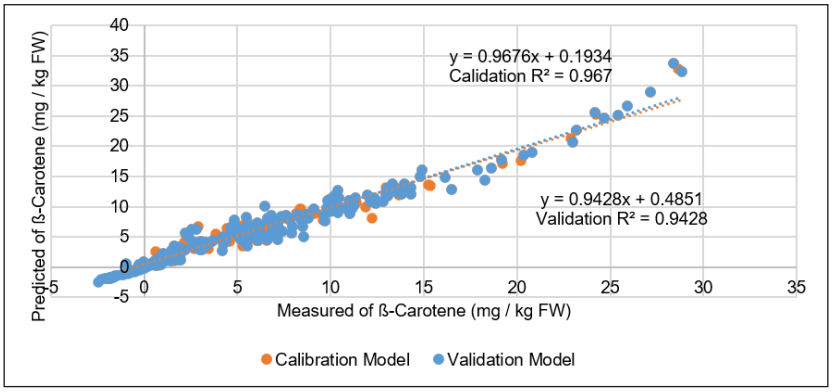

Figure 9. Scatter plots of measured versus predicted β-carotene concentrations in bronzed jackfruit flesh at 12 weeks after anthesis using Vis-NIR reflectance spectra

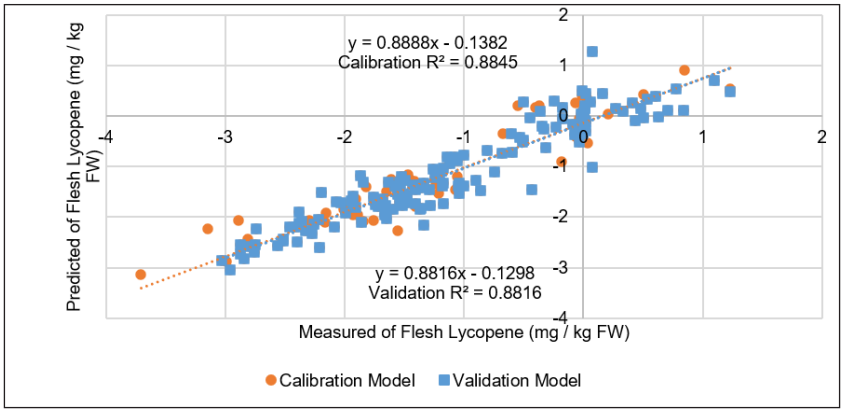

Figure 10. Scatter plots of measured versus predicted lycopene concentrations in normal jackfruit flesh at 14 WAA using Vis-NIR reflectance spectra

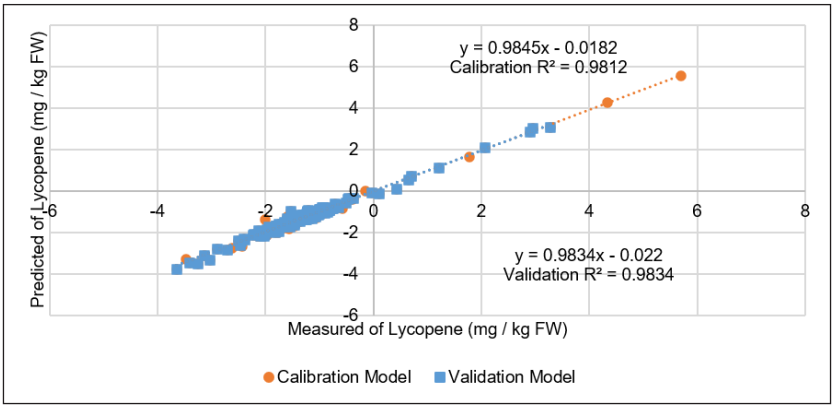

Figure 11. Scatter plots of measured versus predicted lycopene concentrations in bronzed jackfruit flesh at 14 WAA using Vis-NIR reflectance spectra

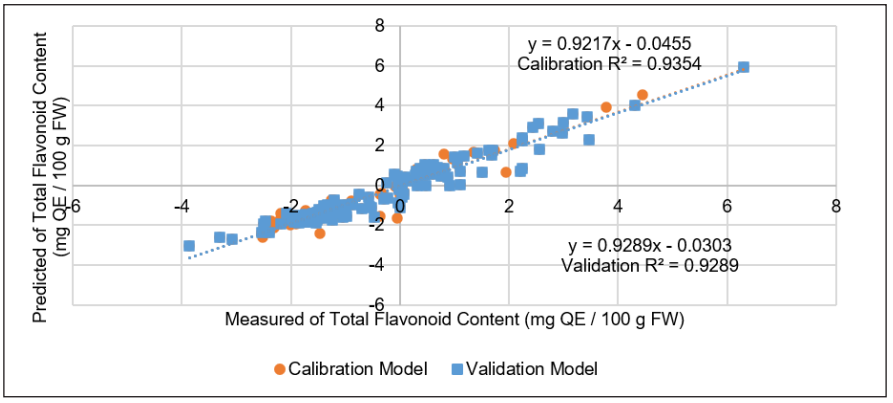

Figure 12. Scatter plots of measured versus predicted total flavonoid content in normal jackfruit flesh at 14 WAA using reflectance spectral data

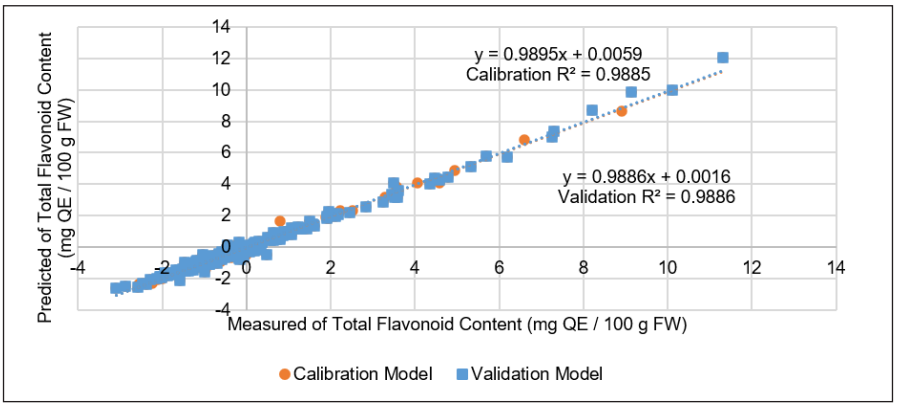

Figure 13. Scatter plots of measured versus predicted total flavonoid content in bronzed jackfruit flesh at 14 WAA using reflectance spectral data

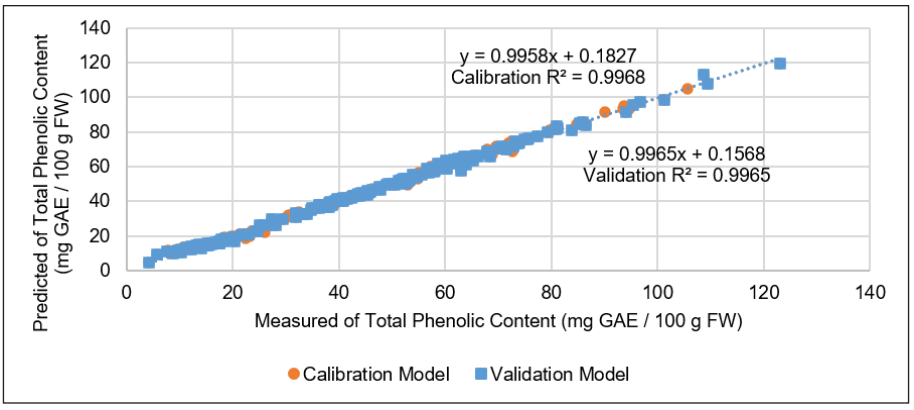

Figure 14. Scatter plots of measured versus predicted total phenolic content in normal jackfruit flesh at 12 WAA using reflectance spectral data

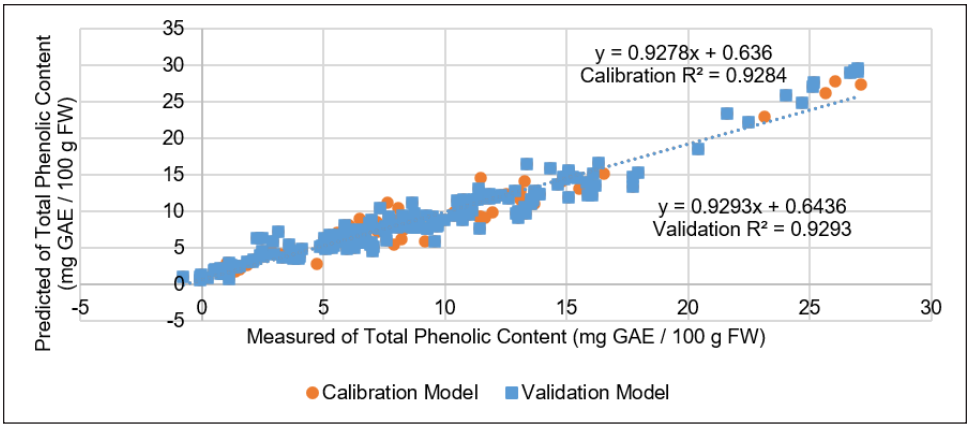

Figure 15. Scatter plots of measured versus predicted total phenolic content in bronzed jackfruit flesh at 12 WAA using reflectance spectral data

PLSR Prediction of Biochemical Attributes

β-Carotene Prediction at 12 and 14 WAA

The PLSR models for β-carotene showed different prediction performance across maturity stages and fruit conditions (Table 3). At 12 WAA, the selected model for normal fruit produced an Rc^2 of 0.95, Rp^2 of 0.88, RMSEP of 1.71, and RPD of 4.12. The corresponding model for bronzing-affected fruit produced Rc^2 of 0.89, Rp^2 of 0.90, RMSEP of 1.99, and RPD of 2.26. The correlation values were above 0.94, while the bias values ranged from -0.20 to 0.16.

At 14 WAA, the normal-fruit model produced Rc^2 of 0.98, Rp^2 of 0.98, RMSEP of 1.35, and RPD of 1.67. For bronzing-affected fruit, the model produced Rc^2 of 0.96, Rp^2 of 0.91, RMSEP of 0.89, and RPD of 4.12. Thus, the prediction results did not show a consistent change with increasing maturity or with fruit condition.

Lycopene Prediction at 14 WAA

Lycopene prediction was evaluated at 14 WAA for both normal and bronzing-affected fruit (Table 4). The selected model for normal fruit produced Rc^2 of 0.98, Rp^2 of 0.99, RMSEP of 1.17, and RPD of 1.47. For bronzing-affected fruit, the corresponding values were Rc^2 of 0.98, Rp^2 of 0.94, RMSEP of 0.22, and RPD of 12.36.

The RPD obtained for bronzing-affected fruit was considerably higher than that obtained for normal fruit. However, RPD is influenced by both prediction error and the spread of the reference values. Therefore, the high RPD should be considered together with Rp^2, RMSEP, bias, and the independent validation data rather than being interpreted on its own.

Table 3
Summary of PLSR results for β-carotene content prediction in jackfruit (cv. Tekam Yellow) at different fruit conditions and maturity stages (weeks after anthesis)

He	Wa	Means	SDe	Rc^2	RMSEc	Rp^2	RMSEp	Bi	Slo	Off	Corr	RPDe
No	12	6.39a	7.05	0.95	0.20	0.88	1.71	-0.20	0.92	0.40	0.94	4.12
Br	12	4.69b	4.49	0.89	1.99	0.90	1.99	0.16	0.91	0.95	0.95	2.26
No	14	5.09b	2.25	0.98	1.44	0.98	1.35	-0.19	0.99	-0.11	0.99	1.67
Br	14	3.02c	3.67	0.96	0.79	0.91	0.89	-0.08	0.91	0.20	0.95	4.12

Note. He = Fruit condition, No = Normal, Br = Bronzing, Wa = week after anthesis, SDe = standard deviation, Bi = bias, Slo = slope, Off = offset, Corr = correlation, RPDe = residual prediction deviation

Table 4
Summary of PLSR results for lycopene prediction in jackfruit (cv. Tekam Yellow) flesh at 14 weeks after anthesis under normal and bronzed conditions.

He	Wa	Means	SDe	Rc^2	RMSEc	Rp^2	RMSEp	Bi	Slo	Off	Corr	RPDe
No	14	2.98a	1.72	0.98	1.26	0.99	1.17	-0.15	0.99	-0.10	0.99	1.47
Br	14	2.21ab	2.72	0.98	0.19	0.94	0.22	0.01	0.89	-0.14	0.97	12.36

Note. He = Fruit condition, No = Normal, Br = Bronzing, Wa = week after anthesis, SDe = standard deviation, Bi =bias, Slo = slope, Off = offset, Corr = correlation, RPDe = residual prediction deviation

Total Flavonoid Content Prediction

The TFC models showed useful statistical relationships at several maturity stages, although the selected preprocessing treatment and number of latent variables differed between maturity stages and fruit conditions (Table 5).

At 10 WAA, the normal-fruit model produced Rp^2 of 0.98 and RPD of 43.17, while the bronzing-affected model produced Rp^2 of 0.87 and RPD of 14.49. At 12 WAA, Rp^2 values of 0.80 and 0.90 were obtained for normal and bronzing-affected fruit, respectively, with corresponding RPD values of 10.00 and 17.92. At 14 WAA, the normal-fruit model produced Rp^2 of 0.93 and RPD of 3.36, whereas the bronzing-affected model produced Rp^2 of 0.97 and RPD of 28.78.

The results indicate that TFC was statistically related to the rind spectral measurements under several of the conditions examined. Nevertheless, the large variation in RPD values means that the prediction results should be considered together with the other validation statistics and the distribution of the reference values.

Total Phenolic Content Prediction at 10 and 12 WAA

TPC prediction showed greater variation than TFC prediction (Table 6). At 10 WAA, the normal-fruit model produced Rp^2 of 0.99, RMSEP of 1.39, and RPD of 0.87. The bronzing-affected model produced Rp^2 of 0.87, RMSEP of 2.10, and RPD of 1.97

At 12 WAA, prediction performance improved for both fruit conditions. The normal-fruit model achieved Rc^2 of 0.94, Rp^2 of 0.87, RMSEP of 1.84, and RPD of 3.57. The bronzing-affected model produced Rc^2 of 0.94, Rp^2 of 0.92, RMSEP of 1.79, and RPD of 2.54. These results indicate that TPC prediction was affected by both maturity stage and fruit condition.

Comparative Interpretation of PLSR Performance

Prediction performance differed among biochemical attributes, maturity stages, fruit conditions, and spectral preprocessing treatments. Preprocessing combinations involving smoothing and scatter correction, particularly SG-SNV and related combinations, gave stable results for several of the models.

The effect of bronzing was not consistent across all attributes. Some models developed for bronzing-affected fruit produced higher Rp^2 or RPD values than the corresponding normal-fruit models, whereas other models showed lower performance. Therefore, the presence of bronzing did not result in a consistent increase or decrease in model performance.

Among the biochemical attributes examined, the stronger statistical relationships were obtained for selected β-carotene, lycopene, and TFC models, while TPC prediction

Table 5
Performance of PLSR models for predicting total flavonoid content in jackfruit (cv. Tekam Yellow) flesh at 10, 12, and 14 weeks after anthesis under normal and bronzed conditions

He	Wa	Means	SDe	Rc^2	RMSEc	Rp^2	RMSEp	Bi	Slo	Off	Corr	RPDe
No	10	11.28ab	10.36	0.99	0.23	0.98	0.24	0.07	0.98	0.07	0.99	43.17
Br	10	6,22d	6.52	0.95	0.38	0.87	0.45	0.00	0.86	-0.10	0.93	14.49
No	12	7.34cd	7.30	0.91	0.54	0.80	0.73	-0.06	0.81	-0.16	0.89	10.00
Br	12	9.31bc	6.81	0.75	0.62	0.90	0.38	0.11	0.98	0.10	0.96	17.92
No	14	9.69b	9.20	0.95	2.53	0.93	2.74	-0.04	0.94	0.37	0.96	3.36
Br	14	12.36a	10.65	0.98	0.30	0.97	0.37	-0.02	0.98	-0.02	0.99	28.78

Note. He = Fruit condition, No = Normal, Br = Bronzing, Wa = week after anthesis, SDe = standard deviation, Bi =bias, Slo = slope, Off = offset, Corr = correlation, RPDe = residual prediction deviation

Table 6
Performance of PLSR models for predicting total phenolic content in jackfruit (cv. Tekam Yellow) flesh at 10 and 12 weeks after anthesis under normal and bronzed conditions

He	Wa	Means	SDe	Rc^2	RMSEc	Rp^2	RMSEp	Bi	Slo	Off	Corr	RPDe
No	10	2.81c	1.21	0.99	1.48	0.99	1.39	0.10	0.99	0.65	1.00	0.87
Br	10	4.05b	4.14	0.92	1.71	0.87	2.10	0.13	0.78	2.15	0.94	1.97
No	12	8.00a	6.56	0.94	1.31	0.87	1.84	-0.16	0.88	0.72	0.94	3.57
Br	12	4.19b	4.55	0.94	1.53	0.92	1.79	-0.06	0.91	0.80	0.96	2.54

Note. He = Fruit condition, No = Normal, Br = Bronzing, Wa = week after anthesis, SDe = standard deviation, Bi =bias, Slo = slope, Off = offset, Corr = correlation, RPDe = residual prediction deviation

showed greater variation. The use of 30 scanning positions per fruit also provided a broader representation of spatial variation across the heterogeneous rind.

The results show that rind-acquired Vis-NIR spectra can be statistically related to biochemical attributes measured in the flesh. These models should be regarded as indirect predictions based on relationships between external spectral variation and internal biochemical variation, rather than as direct optical measurements of flesh constituents.

DISCUSSION

Maturity- and Bronzing-Associated Biochemical Changes

Maturity stage and fruit condition affected the biochemical composition of Tekam Yellow jackfruit, but the responses varied across the four attributes. The significant WAA × fruit condition interaction for β-carotene shows that the difference between normal and bronzing-affected fruit changed during fruit development. At the later maturity stages, normal fruit generally contained more β-carotene than bronzing-affected fruit. This pattern is consistent with changes in pigment composition that occur during jackfruit maturation and ripening (Kaur et al., 2024). The lower β-carotene content observed in bronzing-affected fruit may be related to changes in pigment stability under physiological stress. However, the present study did not investigate carotenoid biosynthesis, degradation, or related metabolic pathways, so this explanation remains tentative.

Lycopene followed a somewhat different pattern. Maturity stage significantly affected lycopene concentration, but the interaction between WAA and fruit condition was not significant. Bronzing-affected fruit nevertheless had lower mean lycopene values than normal fruit. This difference suggests that β-carotene and lycopene did not respond in exactly the same way during fruit development or under bronzing-associated physiological changes. Previous studies in other fruit systems have shown that visible/NIR spectroscopy can provide useful information related to carotenoid content (Clément et al., 2015; Tilahun et al., 2018a).

TFC and TPC were both affected by the interaction between maturity stage and fruit condition. The changes in these antioxidant-related attributes may be associated with changes in secondary metabolism during fruit development and physiological stress (Ding & Syazwani, 2016; Lin et al., 2016; Wulandari et al., 2020). Biotic stress can also alter cellular redox balance and antioxidant metabolism through the production and regulation of reactive oxygen species (Sahu et al., 2022). Nevertheless, the present measurements only describe differences in biochemical composition. They do not provide direct evidence for a particular metabolic pathway associated with bronzing.

The variation observed in the reference measurements was also important for the spectroscopic analysis. Differences among maturity stages and fruit conditions provided the range of biochemical values required to establish and test the PLSR relationships. Without

sufficient variation in the reference data, a regression model may show apparently good statistical fit without being useful across a wider population.

Spectral Characteristics and Preprocessing

The rind spectra contained broad, overlapping features, along with baseline variation and scattering effects. This type of spectral response is common in intact fruit because the measured signal is influenced not only by chemical composition but also by tissue structure and other physical properties (Lim et al., 2026c; Nicolaï et al., 2007). The rough and uneven surface of jackfruit rind can further increase variation between scanning positions.

The spectral regions around 760 and 970 nm were mainly associated with O-H-related responses, particularly those related to water. Similar water-related spectral behaviour has been reported in fruit and jackfruit studies (Babu et al., 2020; Maniwara et al., 2014; Saechua et al., 2021). These wavelengths should not be interpreted as unique markers for carotenoids, antioxidant compounds, or bronzing. The observed response may instead reflect combined effects of water status, tissue structure, and physiological changes occurring during fruit development.

The broader feature around 970 nm was visible in the measured spectra but was outside the final 500-950 nm modelling range. Within the selected range, regression coefficient profiles indicated contributions from regions around 754-760 nm and toward 945 nm. Because Vis-NIR absorption bands are broad and often overlap, these regions cannot be assigned to a single biochemical compound on the basis of the present data alone.

Spectral preprocessing helped reduce baseline variation, noise, and scattering effects in several of the models. Smoothing combined with SNV or MSC provided useful preprocessing for a number of attributes, which agrees with previous NIR studies of intact fruit (Guthrie et al., 1998; Golic & Walsh, 2006; Lim et al., 2026c; Saranwong et al., 2004). The use of multiple scanning positions was also relevant because jackfruit rind is not spectrally uniform. Measurements from 30 positions across five rind zones therefore gave a broader representation of the surface than would have been obtained from a single measurement location (Li et al., 2023).

Prediction of Carotenoids and Antioxidant Attributes

The PLSR results show that prediction performance depended on the biochemical attribute, maturity stage, and fruit condition. For β-carotene, the normal-fruit model at 12 WAA produced Rp^2 of 0.88 and RPD of 4.12, while the bronzing-affected model produced Rp^2 of 0.90 and RPD of 2.26. At 14 WAA, the normal-fruit model had Rp^2 of 0.98 but RPD of 1.67, whereas the bronzing-affected model had Rp^2 of 0.91 and RPD of 4.12. Thus, a higher Rp^2 did not necessarily correspond to a higher RPD. The differences also show that model behaviour changed with both maturity and fruit condition.

The lycopene results provide another example of why several validation statistics should be examined together. At 14 WAA, the normal-fruit model produced Rp^2 of 0.99 and RPD of 1.47, whereas the bronzing-affected model produced Rp^2 of 0.94 and RPD of 12.36. The high RPD for bronzing-affected fruit is associated with the low prediction error and the distribution of the validation reference values. It should therefore not be taken by itself as evidence that lycopene was directly measured through the rind. Similar visible/NIR approaches have been used to estimate carotenoid-related attributes in other fruit systems (Clément et al., 2015; Lim et al., 2026c; Tilahun et al., 2018a).

TFC showed relatively strong statistical relationships at several maturity stages, but the RPD values varied substantially. The normal-fruit model at 10 WAA, for example, produced Rp^2 of 0.98 and RPD of 43.17, whereas the corresponding bronzing-affected model produced Rp^2 of 0.87 and RPD of 14.49. At 14 WAA, RPD values of 3.36 and 28.78 were obtained for normal and bronzing-affected fruit, respectively. Such large RPD values should be treated carefully because RPD is calculated from the standard deviation of the validation reference values relative to prediction error. A narrow or unevenly distributed validation population can therefore influence the apparent magnitude of RPD.

TPC showed a different pattern. At 10 WAA, the normal-fruit model had Rp^2 of 0.99 but RPD of only 0.87, while the 12-WAA normal-fruit model had Rp^2 of 0.87 and RPD of 3.57. The bronzing-affected model at 12 WAA produced Rp^2 of 0.92 and RPD of 2.54. This difference between Rp^2 and RPD again shows why model performance should not be described using a single statistic. Similar variation in NIR prediction performance has been reported for biochemical attributes in agricultural products (Chaukhande et al., 2024; Clark et al., 2022).

Taken together, the results suggest that rind spectra contain information that can be used to establish statistical relationships with selected internal biochemical measurements. However, the strength of these relationships was condition-dependent. The models therefore should not be presented as universally applicable predictions for all maturity stages or fruit conditions.

Practical Relevance and Limitations

A key limitation of this study is the difference between the location of spectral measurement and the location of the reference measurement. Vis-NIR spectra were collected from the rind, whereas β-carotene, lycopene, TFC, and TPC were measured destructively from the flesh. The resulting models therefore describe relationships between external rind spectral characteristics and internal biochemical attributes. They should not be interpreted as direct optical measurements of the compounds present in the flesh.

Previous jackfruit studies have shown that skin-surface NIR measurements can provide information related to internal physicochemical properties. Abdullah (2019) investigated

shortwave NIR spectroscopy for jackfruit quality attributes, while Abdullah et al. (2018, 2021) reported prediction of moisture and soluble solids content using skin-surface spectra. These studies support the feasibility of indirect surface-based assessment, but they do not establish a specific optical penetration depth through the rind of Tekam Yellow under the conditions used in the present study.

Rind thickness may also affect the interaction between the incident radiation and the fruit tissue. However, rind thickness was not measured in this experiment. In the previous morphological and physical characterisation of Tekam Yellow, flesh thickness varied with maturity stage and fruit condition, whereas rind thickness was not reported (Lim et al., 2026a). Rind thickness should therefore be considered a possible source of spectral variation, although its contribution to the current models cannot be quantified from the available measurements.

The disease literature provides the biological context for jackfruit bronzing. Bronzing was reported as an emerging disease in Peninsular Malaysia in association with *Pantoea stewartii* subsp. *stewartii* (Zulperi et al., 2017), and subsequent molecular work supported this association (Ibrahim et al., 2020). Bronzing has also been reported in other jackfruit-producing regions, including China (Zhao et al., 2023). The present study, however, did not directly detect *P. stewartii* subsp. *stewartii* and did not develop a pathogen diagnostic test. The spectroscopic models were developed for biochemical prediction, so the observed spectral relationships should not be interpreted as direct pathogen detection or confirmation of bronzing disease.

The variation in model performance also points to the need for broader validation. NIR model robustness can be affected by biological variation, particularly when the calibration population is relatively limited (Bobelyn et al., 2010; Lim et al., 2026b; Peirs et al., 2003). Future work should include larger numbers of fruits from different seasons, orchards, cultivars, maturity stages, and levels of bronzing severity. Independent external validation would also be needed to determine whether the relationships observed in the present dataset can be transferred to other production conditions.

Measurements at different tissue depths or studies involving separate rind and internal tissue layers could further clarify the relationship between surface spectra and internal biochemical variation. For practical development, future calibration datasets should also contain sufficient representation of both healthy and bronzing-affected fruit across the relevant biochemical range. Recalibration may be necessary when the model is applied under different seasonal or production conditions.

Multi-position rind-based Vis-NIRS combined with PLSR provides a possible rapid screening approach for selected internal biochemical attributes of intact Tekam Yellow jackfruit. Its usefulness depends on the target attribute, maturity stage, fruit condition, preprocessing method, and reference-value distribution. The approach should therefore

be considered a potential indirect screening method rather than a direct measurement or diagnostic technique.

CONCLUSION

This study examined changes in selected carotenoid and antioxidant-related attributes of Tekam Yellow jackfruit at 10, 12, and 14 weeks after anthesis under normal and bronzing-affected conditions. β-Carotene, lycopene, TFC, and TPC showed different responses to maturity stage and fruit condition, providing a useful range of reference values for spectroscopic modelling.

Rind-acquired Vis-NIR spectra combined with PLSR were able to establish statistical relationships with selected biochemical attributes measured in the flesh. Prediction performance varied with the target attribute, maturity stage, fruit condition, and spectral preprocessing. The β-carotene model for normal fruit at 12 WAA produced Rp^2 of 0.88 and RPD of 4.12, while selected TFC and lycopene models also showed strong statistical relationships. For TPC at 12 WAA, Rp^2 values of 0.87 and 0.92 were obtained for normal and bronzing-affected fruit, respectively, with RPD values of 3.57 and 2.54.

The spectral responses around 760 and 945 nm contributed to several of the regression models, whereas the broader feature near 970 nm was mainly associated with water-related absorption and was outside the final modelling range. These wavelength regions should not be regarded as unique spectral signatures of individual biochemical compounds or bronzing.

The present findings support the use of multi-position rind-based Vis-NIRS as a potential non-destructive screening approach for selected internal biochemical attributes of intact Tekam Yellow jackfruit. However, the models represent indirect relationships between rind spectra and flesh measurements and should not be interpreted as direct measurement of internal compounds or as detection of *Pantoea stewartii* subsp. *stewartii*. The study was limited to one cultivar, three maturity stages, and the sampled production conditions. Larger datasets covering additional cultivars, seasons, orchards, maturity stages, and levels of bronzing severity, together with independent external validation, are needed before the models can be considered for wider practical application.

Data Availability Declaration

The datasets generated during and/or analyzed during the current study are available.

Funding Declaration

This research did not receive any specific grant from funding agencies in the public, commercial, or not-for-profit sectors.

Declaration of Competing Interest

The authors declare that there are no known financial conflicts of interest or personal relationships that could have influenced the research, analysis, or interpretation of the data presented in this manuscript.

ACKNOWLEDGEMENT

The authors sincerely express their gratitude to the Department of Crop Science, Faculty of Agriculture; the Department of Biological and Agricultural Engineering, Faculty of Engineering; and the Institute of Plantation Studies at Universiti Putra Malaysia for their invaluable technical assistance and logistical support throughout this research.

REFERENCES

Abdullah, N. (2019). *Application of shortwave near infrared spectroscopy in determining physicochemical properties of jackfruit* [Master's thesis, Universiti Putra Malaysia].

Abdullah, N., Nawi, N. M., Ding, P., Kassim, M. S. M., & Lazim, S. S. R. M. (2018). Preliminary study to predict moisture content of jackfruit skin using shortwave near infrared spectroscopy. *Food Research, 3*(2), 128-132. https://doi.org/10.26656/fr.2017.3(2).135

Abdullah, N., Nawi, N. M., Ding, P., Kassim, M. S. M., & Lazim, S. S. R. M. (2021). Prediction of soluble solids content of jackfruit from skin surface using spectroscopic method. *Agricultural Mechanization in Asia, Africa and Latin America, 52*(3), 4013-4021.

Abidin, N., Ismail, S. I., Vadamalai, G., Yusof, M. T., Hakiman, M., Karam, D. S., Ismail-Suhaimy, N. W., Ibrahim, R., & Zulperi, D. (2020). Genetic diversity of *Pantoea stewartii* subspecies *stewartii* causing jackfruit-bronzing disease in Malaysia. *PLOS ONE, 15*(6), Article e0234350. https://doi.org/10.1371/journal.pone.0234350

Abidin, N., Ismail, S. I., Vadamalai, G., Yusof, M. T., Hakiman, M., Karam, D. S., & Zulperi, D. (2021). Pathogenic variability of the jackfruit-bronzing bacterium *Pantoea stewartii* subspecies *stewartii* infection to jackfruit varieties and its pivotal plant hosts in Malaysia. *Agronomy, 11*(11), Article 2113. https://doi.org/10.3390/agronomy11112113

Abu Bakar, M. F., Mohamed, M., Rahmat, A., & Fry, J. (2009). Phytochemicals and antioxidant activity of different parts of bambangan (*Mangifera pajang*) and tarap (*Artocarpus odoratissimus*). *Food Chemistry, 113*, 479-483. https://doi.org/10.1016/j.foodchem.2008.07.081

Ali, M. M., Hashim, N., & Shahamshah, M. I. (2021). Durian (*Durio zibethinus*) ripeness detection using thermal imaging with multivariate analysis. *Postharvest Biology and Technology, 176*, Article 111517. https://doi.org/10.1016/j.postharvbio.2021.111517

Babu, P. S., Sudheer, K. P., Sarathjith, M. C., Mathew, S. M., & Gopinath, G. (2020). Quality evaluation of tender jackfruit using near-infrared reflectance spectroscopy. *Journal of Applied Horticulture, 22*(3), 171-175. https://doi.org/10.37855/jah.2020.v22i03.31

Bobelyn, E., Serban, A., Nicu, M., Lammertyn, J., Nicolaï, B. M., & Saeys, W. (2010). Postharvest quality of apple predicted by NIR spectroscopy: Study of the effect of biological variability on spectra and model performance. *Postharvest Biology and Technology, 55*(3), 133-143. https://doi.org/10.1016/j.postharvbio.2009.09.006

Chaukhande, P., Luthra, S. K., Patel, R. N., Padhi, S. R., Mankar, P., Mangal, M., & Riar, A. S. (2024). Development and validation of near-infrared reflectance spectroscopy prediction modeling for the rapid estimation of biochemical traits in potato. *Foods, 13*(11), Article 1655. https://doi.org/10.3390/foods13111655

Clark, C. J., McGlone, V. A., De Silva, H. N., Manning, M. A., Burdon, J., & Mowat, A. D. (2004). Prediction of storage disorders of kiwifruit (*Actinidia chinensis*) based on visible-NIR spectral characteristics at harvest. *Postharvest Biology and Technology, 32*(2), 147-158. https://doi.org/10.1016/j.postharvbio.2003.11.004

Clark, C. J., MacFall, J. S., & Rutherfurd, S. M. (2022). Application of near-infrared spectroscopy for rapid non-destructive assessment of tropical fruit quality. *Postharvest Biology and Technology, 188*, Article 111908. https://doi.org/10.1016/j.postharvbio.2022.111908

Clément, A., Bacon, R., Sirois, S., & Dorais, M. (2015). Mature-ripe tomato spectral classification according to lycopene content and fruit type by visible, NIR reflectance and intrinsic fluorescence. *Quality Assurance and Safety of Crops & Foods, 7*(5), 747-756. https://doi.org/10.3920/QAS2014.0521

Ding, P., & Syazwani, S. (2016). Physicochemical quality, antioxidant compounds and activity of MD-2 pineapple fruit at five ripening stages. *International Food Research Journal, 23*(2), 549-555. http://core.ac.uk/download/pdf/153810846.pdf

Golic, M., & Walsh, K. B. (2006). Robustness of calibration models based on near infrared spectroscopy for the in-line grading of stonefruit for total soluble solids content. *Analytica Chimica Acta, 555*(2), 286-291. https://doi.org/10.1016/j.aca.2005.09.014

Guthrie, J., Wedding, B., & Walsh, K. (1998). Robustness of NIR calibrations for soluble solids in intact melon and pineapple. *Journal of Near Infrared Spectroscopy, 6*(1), 259-265. https://doi.org/10.1255/jnirs.112

Ibrahim, R., Ismail-Suhaimy, N. W., Shu-Qing, T., Ismail, S. I., Abidin, N., Hakiman, M., Karam, D. S., Ahmad-Hamdani, M. S., Yusof, M. T., & Zulperi, D. (2020). Molecular characterization and phylogenetic analysis of *Pantoea stewartii* subspecies *stewartii* causing bronzing disease of jackfruit in Malaysia based on *cps* and *hrp* gene sequences. *Journal of Plant Pathology, 102*(1), 193-199. https://doi.org/10.1007/s42161-019-00383-7

Jarman, S., Carr, T., Hampel-Arias, Z., Flynn, E., & Moon, K. (2023). Ensemble segmentation for improved background estimation and gas plume identification in hyperspectral images. In *Applications of machine learning 2023* (Vol. 12675, pp. 41-58). SPIE. https://doi.org/10.1117/12.2677729

Kaur, J., Singh, Z., Mazhar, M. S., Shah, H. M. S., & Woodward, A. (2024). Changes in physical attributes, activities of fruit softening enzymes, cell wall polysaccharides and fruit quality of jackfruit (*Artocarpus heterophyllus* Lam.) as influenced by maturation and ripening. *Horticulturae, 10*(12), Article 1264. https://doi.org/10.3390/horticulturae10121264

Li, J., Zhang, Y., Zhang, Q., Duan, D., & Chen, L. (2023). Establishment of a multi-position general model for evaluation of water core and soluble solid content in 'Fuji' apples using on-line full-transmittance

visible and near infrared spectroscopy. *Journal of Food Composition and Analysis, 117*, Article 105150. https://doi.org/10.1016/j.jfca.2023.105150

Lim, K. J., Ding, P., Nawi, N. M., & Jusoh, M. (2026a). Morphological and physical characterization of bronzing-affected jackfruit (*Artocarpus heterophyllus* Lam. cv. Tekam Yellow) across maturity stages: Influence of rind and flesh attributes. *Journal of Food Science, 91*(4), Article e71075. https://doi.org/10.1111/1750-3841.71075

Lim, K. J., Ding, P., Nawi, N. M., Jusoh, M., Abdullah, N., & Lazim, S. S. R. M. (2026b). Predicting the soluble solid concentration and ascorbic acid of intact jackfruit var. Tekam Yellow using visible-near-infrared spectroscopy: Comparison of rind and flesh. *Food Analytical Methods, 19*(8), Article 218. https://doi.org/10.1007/s12161-026-03129-1

Lim, K. J., Ding, P., Nawi, N. M., Jusoh, M., & Khuzaimah, Z. (2026c). Comparative evaluation of hyperspectral, thermal, and near-infrared imaging systems for non-destructive prediction of fruit and vegetable quality: A review. *Journal of Nondestructive Evaluation, 45*, Article 79. https://doi.org/10.1007/s10921-026-01376-0

Lim, K. J., Ding, P., Nawi, N. M., & Jusoh, M. (2026d). Robust non-destructive prediction of color attributes associated with bronzing in jackfruit (*Artocarpus heterophyllus* cv. 'Tekam Yellow') using visible-near infrared spectroscopy. *Applied Fruit Science, 68*(4), Article 217. https://doi.org/10.1007/s10341-026-01925-x

Lin, D., Xiao, M., Zhao, J., Li, Z., Xing, B., Li, X., & Chen, S. (2016). An overview of plant phenolic compounds and their importance in human nutrition and management of type 2 diabetes. *Molecules, 21*(10), Article 1374. https://doi.org/10.3390/molecules21101374

Maniwara, P., Nakano, K., Boonyakiat, D., Ohashi, S., Hiroi, M., & Tohyama, T. (2014). The use of visible and near infrared spectroscopy for evaluating passion fruit postharvest quality. *Journal of Food Engineering, 143*, 33-43. https://doi.org/10.1016/j.jfoodeng.2014.06.028

Mijin, S., & Ding, P. (2020). Growth development and structural changes of Malaysian jackfruit cv. Tekam Yellow syncarp. *Scientia Horticulturae, 272*, Article 109594. https://doi.org/10.1016/j.scienta.2020.109594

Mijin, S., Ding, P., Saari, N., & Ramlee, S. I. (2021). Effects of pollination techniques and harvesting stage on the physico-chemical characteristics of jackfruit. *Scientia Horticulturae, 285*, Article 110199. https://doi.org/10.1016/j.scienta.2021.110199

Musa, K. H., Abdullah, A., Jusoh, K., & Subramaniam, V. (2011). Antioxidant activity of pink flesh guava (*Psidium guajava* L.): Effect of extraction techniques and solvents. *Food Analytical Methods, 4*(1), 100-107. https://doi.org/10.1007/s12161-010-9139-3

Nagata, M., & Yamashita, I. (1992). Simple method for simultaneous determination of chlorophyll and carotenoids in tomato fruit. *Journal of the Japanese Society for Food Science and Technology, 39*(10), 925-928. https://doi.org/10.3136/nskkk1962.39.925

Nagy, A., Riczu, P., & Tamas, J. (2016). Spectral evaluation of apple fruit ripening and pigment content alteration. *Scientia Horticulturae, 201*, 256-264. https://doi.org/10.1016/j.scienta.2016.02.016

Nicolaï, B. M., Beullens, K., Bobelyn, E., Peirs, A., Saeys, W., & Theron, K. I. (2007). Non-destructive measurement of fruit and vegetable quality by means of NIR spectroscopy: A review. *Postharvest Biology and Technology, 46*(2), 99-118. https://doi.org/10.1016/j.postharvbio.2007.06.024

Peirs, A., Tirry, J., Verlinden, B., Darius, P., & Nicolaï, B. M. (2003). Effect of biological variability on the robustness of NIR models for soluble solids content of apples. *Postharvest Biology and Technology, 28*(2), 269-280. https://doi.org/10.1016/S0925-5214(02)00196-5

Saechua, W., Sharma, S., Nakawajana, N., Leepaitoon, K., Chunsri, R., Posom, J., & Pornchaloempong, P. (2021). Integrating Vis-SWNIR spectrometer in a conveyor system for in-line measurement of dry matter content and soluble solids content of durian pulp. *Postharvest Biology and Technology, 181*, Article 111640. https://doi.org/10.1016/j.postharvbio.2021.111640

Sahu, P. K., Jayalakshmi, K., Tilgam, J., Gupta, A., Nagaraju, Y., Kumar, A., & Rajawat, M. V. S. (2022). ROS generated from biotic stress: Effects on plants and alleviation by endophytic microbes. *Frontiers in Plant Science, 13*, Article 1042936. https://doi.org/10.3389/fpls.2022.1042936

Saranwong, S., Sornsrivichai, J., & Kawano, S. (2004). Prediction of ripe-stage eating quality of mango fruit from its harvest quality measured nondestructively by near infrared spectroscopy. *Postharvest Biology and Technology, 31*(2), 137-145. https://doi.org/10.1016/j.postharvbio.2003.08.007

Sirisomboon, P., & Nawayon, J. (2017). Evaluation of soluble solids of curry soup containing coconut milk by near infrared spectroscopy. *Journal of Near Infrared Spectroscopy, 25*(3), 203-210. https://doi.org/10.1177/0967033517711472

Tilahun, S., Seo, M. H., Hwang, I. G., Kim, S. H., Choi, H. R., & Jeong, C. S. (2018a). Prediction of lycopene and β-carotene in tomatoes by portable chroma-meter and VIS/NIR spectra. *Postharvest Biology and Technology, 136*, 50-56. https://doi.org/10.1016/j.postharvbio.2017.10.007

Wulandari, L., Permana, B. D., & Kristiningrum, N. (2020). Determination of total flavonoid content in medicinal plant leaves powder using infrared spectroscopy and chemometrics. *Indonesian Journal of Chemistry, 20*(5), 1044-1051. https://doi.org/10.22146/ijc.47047

Zhao, Y., Xiao, M., Yan, C. B., Hu, F. C., Zhang, S. Q., Wang, X. H., & Fan, H. Y. (2023). First report of bronzing disease caused by *Pantoea stewartii* on jackfruit in China. *Plant Disease, 107*(8), 2514. https://doi.org/10.1094/PDIS-11-22-2740-PDN

Zulperi, D., Manaf, N., Ismail, S. I., Karam, D. S., & Yusof, M. T. (2017). First report of *Pantoea stewartii* subsp. *stewartii* causing fruit bronzing of jackfruit (*Artocarpus heterophyllus*), a new emerging disease in Peninsular Malaysia. *Plant Disease, 101*(5), 831. https://doi.org/10.1094/PDIS-11-16-1689-PDN